VPS VIBRATIONS IN PHYSICAL SYSTEMS

DOI: 10.21008/j.0860-6897.2021.1.05
Vibrations in Physical Systems, 32(1):2021105, 2021

Stopband Effect and Sound Transmission Loss of Periodic Locally Resonant Structures

Klara JUROS [1,2], Aleksander KRAS[2], Tadeusz KAMISIŃSKI[1]

Corresponding author: Klara JUROS, juros@agh.edu.pl
[1] Akademia Górniczo-Hutnicza w Krakowie, ul. A. Mickiewicza 30, 30-049 Kraków
[2] Silencions Sp. z o.o., ul. Bierutowska 57-59/Budynek 5, 51-317 Wrocław

Abstract This paper investigates the theoretical aspects of sound attenuation of periodic structures with locally resonant elements. The stopband effect in frequency characteristics of infinite periodic structures created by the resonant elements is investigated. The dispersion curves calculation procedure is described in details with the influence of resonance frequency and mass of added locally resonant structure on width of the obtained stopband is investigated. The theoretical formulation for calculation of the sound transmission loss for periodic structure is derived. The performance of the structure with locally resonant elements is evaluated based on dispersion curves obtained for an infinite periodic structure and transmission loss calculated for finite structure is conducted.

Keywords: acoustic metamaterials, periodic structures, locally resonant structures, stopband effect, dispersion curves, transmission loss

1. Introduction

Vibro-acoustic metamaterials are periodic structures which exhibit improved acoustic properties such as sound absorption in low-frequencies, enhanced sound transmission loss or sound insulation, depending on the purpose of the structure [1–3]. An important aspect of metamaterials is their lightweight structure and compact dimensions, especially when it comes to improvement of acoustic properties in low frequency regions [2]. Acoustic metamaterials can be divided in two groups: structures based only on acoustic properties, as Helmholtz resonators [4] and resonant metamaterials, where properties depend on mechanical properties of the designed structure [5]. The considered periodic structures, as indicated by Brillouin [6], can exhibit the so called stop band behavior, where no free wave propagation is possible. The metamaterials with locally resonant elements were firstly exploited only for vibration mitigation but in recent years, the dependencies between stop band behavior in vibrations and sound reduction of the structure are widely investigated [3,7–9].

The goal of this paper it twofold. Firstly to present two methods which can be used for simulation of resonant metamaterials and describing dependency between locally resonant structure parameters as resonance frequency, mass and stop band wideness for two dimensional plate structure. A second goal is to illustrate relationship between two described methods: dispersion diagram and transmission loss of structure.

The study is organized in three parts. Firstly, Section 2 presents the mathematical formulation of the considered metastructure on the two dimensional plate. Section 3 shows the simulation procedure of the transmission loss. Finally, Section 4 summarises and discusses results presented in this study.

2. Theoretical formulation of an infinite periodic structure

The first method for numerical analysis of locally resonant structures, which is the most known method, is the analysis of wave propagation in infinite structure. Infinite structure can be expressed by the analysis of one representative unit cell (UC). If the unit cell is properly defined, it contains all necessary information needed to characterise the infinite structure by applying boundary constraints. In this work, the finite element (FE) method with the use of Transfer Matrix Method is applied to wave propagation analysis in

thin plate structures [5,10]. First of all FE model which later will be used is simulations is described. Second of all, unit cell modelling and application of locally resonant structures is presented.

2.1. FE model formulation

The formulation presented in this work is performed according to Kirchhoff models of thin plate presented in [10–12]. The Kirchhoff plate theory is based on simplified wave equation for elastic wave propagation; with this approximation it can be used only for thin materials and low frequencies. This model considers only flexural waves, without Lamb waves. With this limitation, Kirchhoff model should be used only if thickness of the panel should is at least 10 times larger than analysed wavelengths[13]. In this work the upper frequency limit is 1600 Hz, as this is the highest frequency possible to measure in impedance tube and the plate thickness is 1 mm, therefore the conditions are meet and only flexural waves can be considered.

For unit cell element discretization, the plate was split to 4 nodes square elements, where each of the nodes had 3 degrees of freedom. The derivation of stiffness and mass matrices for square plate elements is based on [12]. One plate element obtain stiffness matrix $\boldsymbol{K}$ as well as mass matrix $\boldsymbol{M}$ of size $N\ x\ N$, where N is total number of degrees of freedom. The matrixes are used in the eigenvalue equation for undamped plate given by:

$$(\boldsymbol{K} - \omega^2 \boldsymbol{M})\boldsymbol{d} = \boldsymbol{0}, \tag{1}$$

where $\boldsymbol{d}$ is a matrix containing nodal displacements and ω is the frequency at which the eigenvalue problem is analysed.

2.2. Unit cell modelling

Unit cell is a representative part of infinite structure, which contain all information needed to characterize the infinite structure. With the use of unit cell modelling the dispersion relations can be obtained. The dispersion relations present how waves of different frequencies propagate in the structure in different directions in the single unit cell. The dispersion relations can be obtained for damped or undamped structures, however the coefficient of damping is neglectable, thus in most cases the undamped model is assumed [9,14]. In this work the dispersion relations are obtained for undamped structure, i.e. for free wave propagation in the material. In thin plate structure, the wave can propagate only in x and y direction and free wave propagation is assumed. The propagation vector can be written as:

$$\boldsymbol{\mu} = [\mu_x, \mu_y] = [0 + i\epsilon_x, 0 + i\epsilon_y], \tag{2}$$

where ϵ_x and ϵ_y are expressed as:

$$[\epsilon_x, \epsilon_y] = [k_x L, k_y L], \tag{3}$$

where k_x and k_y are wavenumbers in x and y direction and L is unit cell length. When the propagation vector is purely imaginary, it means that the wave can propagate between unit cells in structure without any amplitude attenuation [5,10].

In this work unit cell is created from 4 plate elements, where each one has 4 nodes and total of 12 degrees of freedom, as it is presented in [10]. From FE model stiffness and mass matrices are obtained for each plate element. When the unit cell is obtained from several plate elements, global stiffness and mass matrices can be obtained, which contain dependencies between individual nodes in the unit cell [15].

In the unit cell modelling, the periodic boundary condition must be investigated, in order to achieve wave propagation between infinite number of unit cells. In order to characterize stop band phenomena one need to apply Bloch's boundary conditions together with transfer matrix method [10]. In Bloch's theorem one should calculate only displacements in the middle node and on the left and bottom boundary of unit cell. Points placed on the right and top boundary are dependent from the first node group by means of phase shift. The dependency between displacements in unit cell are shown in Fig. 1a and the transfer matrix is given as follows:

$$\boldsymbol{T} = \begin{bmatrix} \boldsymbol{I} & \boldsymbol{0} & \boldsymbol{0} & \boldsymbol{0} & \boldsymbol{0} & \boldsymbol{0} & \boldsymbol{0} & \boldsymbol{0} & \boldsymbol{0} \\ \boldsymbol{0} & \boldsymbol{I} & \boldsymbol{Ie^{ik_xL}} & \boldsymbol{0} & \boldsymbol{0} & \boldsymbol{0} & \boldsymbol{0} & \boldsymbol{0} & \boldsymbol{0} \\ \boldsymbol{0} & \boldsymbol{0} & \boldsymbol{0} & \boldsymbol{I} & \boldsymbol{Ie^{ik_xL}} & \boldsymbol{0} & \boldsymbol{0} & \boldsymbol{0} & \boldsymbol{0} \\ \boldsymbol{0} & \boldsymbol{0} & \boldsymbol{0} & \boldsymbol{0} & \boldsymbol{0} & \boldsymbol{I} & \boldsymbol{Ie^{ik_xL}} & \boldsymbol{Ie^{ik_yL}} & \boldsymbol{Ie^{i(k_x+k_y)L}} \end{bmatrix}. \tag{4}$$

where $\boldsymbol{I}$ is diagonal identity matrix. Transfer matrix $\boldsymbol{T}$ is applied to eigenvalue problem, in order to obtain reduced displacement vector, containing only, in this case, displacements from four nodes and it is done as follows:

$$(\boldsymbol{T}^H \boldsymbol{K}_G \boldsymbol{T} - \omega^2 \boldsymbol{T}^H \boldsymbol{M}_G \boldsymbol{T}) \boldsymbol{d}_{red} = \boldsymbol{0}, \tag{5}$$

where $\boldsymbol{K}_G$ and $\boldsymbol{M}_G$ are global stiffness and mass matrices for the unit cell respectively, and $\boldsymbol{d}_{red}$ is reduced displacement vector.

In order to obtain complete information about wave propagation in infinite structure it is necessary to solve the eigenvalue problem for all pairs (ϵ_x, ϵ_y) belonging to Brillouin zone presented in Fig. 1b. If the unit cell is symmetric the Brillouin zone consists three vectors: $\Gamma(0,0) \rightarrow X(\pi, 0) \rightarrow M(\pi, \pi) \rightarrow \Gamma(0,0)$, and it is called irreducible Brillouin zone. Solving eigenvalue problem for all (ϵ_x, ϵ_y) belonging to irreducible Brillouin zone, frequency zones of free wave propagation are obtained. Frequencies, that are not solution of the eigenvalue problem for any of the (ϵ_x, ϵ_y) are frequencies at which the waves cannot propagate.

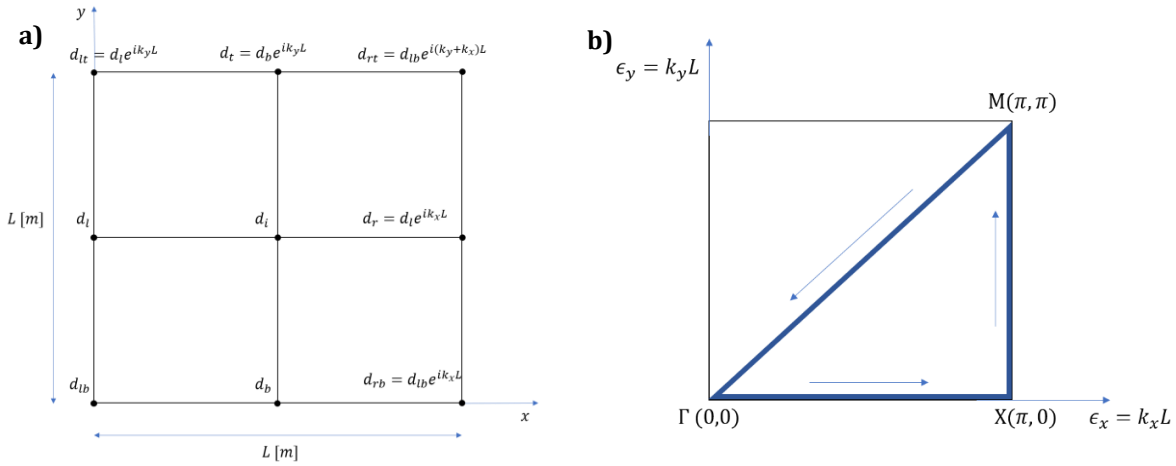

Fig. 1. Depiction of unit cell with FEM mesh with Bloch theorem applied to nodal displacements (a), Brillouin zone in unit cell with three contour vectors marked (b).

In the Fig. 2 the dispersion relation for infinite plain plate is presented. The x-axis represents propagation vector on the irreducible Brillouin contour and the y-axis represents normalized frequency given by:

$$\Omega = \frac{\omega}{\omega_B}, \tag{6}$$

where ω is the outcome of the eigenvalue problem, and ω_B depict Bragg frequency, for which the half of the length of a flexural wave is equal to length of the unit cell. This makes the dispersion curves independent from the unit cell length.

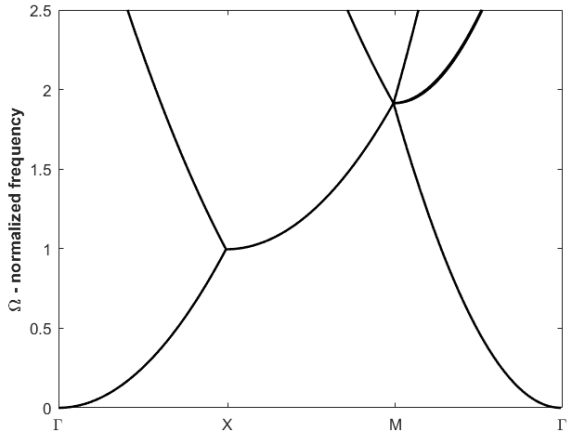

Fig. 2. Dispersion curves for infinite plain plate.

Bragg frequency can be expressed as follows:

$$\omega_B = \frac{2\pi^2}{2L^2}\sqrt{\frac{h^2 E}{12\rho(1-\nu^2)}}, \tag{7}$$

where L is length of unit cell, h thickness of the plate, E Young modulus of material, ρ density and ν is Poisson ratio.

2.3. Locally resonant structures

The stop band effect can be generated through an addition of locally resonant structures (LRS) to unit cell geometry. The most common way is the addition of mass-spring resonator in the middle of the unit cell [5,9,10]. Periodically distributed resonant structures create stopband effect in the area of its resonance frequency. Application of LRS to unit cell requires an additional degree of freedom associated with the spring-mass resonator. Thus, global mass matrix and global stiffness matrix has to be expanded by one row as follows:

$$\widetilde{\boldsymbol{M}_G} = \begin{bmatrix} 0 & \mathbf{0} \\ \mathbf{0} & \boldsymbol{M}_G \end{bmatrix}, \tag{8}$$

$$\widetilde{\boldsymbol{K}_G} = \begin{bmatrix} 0 & \mathbf{0} \\ \mathbf{0} & \boldsymbol{K}_G \end{bmatrix}. \tag{9}$$

Modified global matrices need to be combined with resonator mass and stiffness parameters as follows:

$$\widetilde{\boldsymbol{M}_G}(1,1) = m_{LRS}, \tag{10}$$

$$\widetilde{\boldsymbol{K}_G}(1,1) = \widetilde{\boldsymbol{K}_G}(i,i) = k_{LRS}, \tag{11}$$

$$\widetilde{\boldsymbol{K}_G}(1,i) = \widetilde{\boldsymbol{K}_G}(i,1) = -k_{LRS}, \tag{12}$$

where m_{LRS} and k_{LRS} stands for suspended mass and stiffness of resonator respectively, and i is index of middle node of the unit cell, where the LRS is attached. In the Fig. 3 two charts with dispersion curves are presented and they differ in resonance frequency of LRS and its mass. Resonant frequency f_{LRS} as well as m_{LRS} are presented in reference to Bragg frequency and mass of the plain plate respectively. As one can see in the charts, the wideness of the stopband is variable and it depends on frequency of LRS and on added mass. The limitation of locally resonant structures is the Bragg frequency – above it the stopband effect do not work anymore.

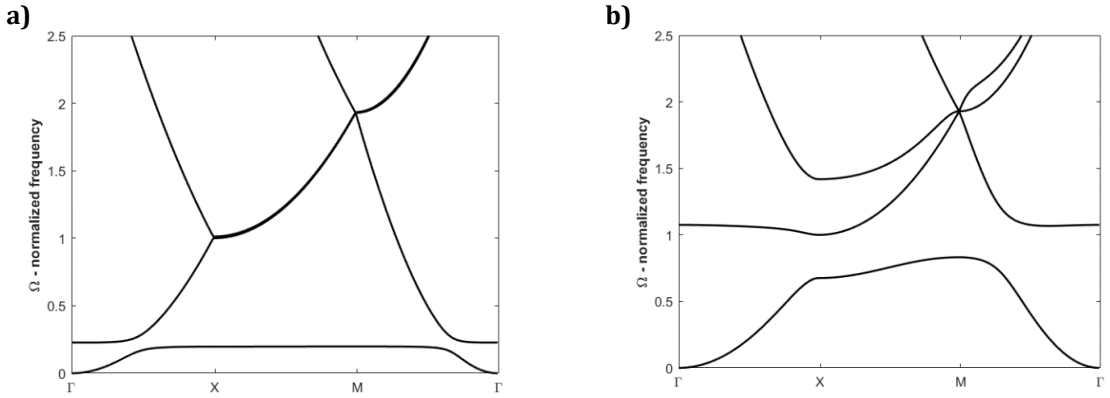

Fig. 3. Dispersion curves for unit cell with added LRS considering $\omega_{LRS} = 0.2\omega_B, m_{LRS} = 0.3m_{plate}$ (a) and $\omega_{LRS} = \omega_B, m_{LRS} = 0.3m_{plate}$ (b).

3. Transmission loss

In this section the acoustic Transmission Loss (TL) of locally resonant structures (LRS) is presented. The mass law is commonly used approximation for predicting the TL of a structure. It assumes that panel has negligible bending and shear stiffness and the structure has no damping [16].
In this work the sound wave perpendicular to structure is assumed, therefore TL can be expressed as follows:

$$TL = 10\log\left[1 + \left(\frac{\pi f M}{\rho_a c_a}\right)^2\right], \tag{13}$$

where M is the mass of the structure, ρ_a is air density, c_a is sound wave velocity in air, and f is frequency. For plain homogenic structure, the TL increases about 6 dB for every octave. The TL calculated from mass law does not take into account the stiffness of single plate, which would increase the TL in low frequency region. The TL of plain structure with LRS does not need periodic boundary condition, as it was considered in section 2 for dispersion calculation. If the ratio between plate area and number of used resonators will be constant, the transmission loss will be also constant. In order to calculate the TL of structure with LRS, mass matrix has to be defined as follows [8,16]:

$$\boldsymbol{M_l} = \begin{bmatrix} m_{plate} & 0 & \cdots & 0 \\ 0 & m_{r_1} & \cdots & 0 \\ \vdots & \vdots & \ddots & \cdots \\ 0 & 0 & 0 & m_{r_n} \end{bmatrix}, \tag{14}$$

where m_{plate} stands for total mass of the plain plate and m_{rn} stands for mass of next LRS. Subsequently, the stiffness matrix must be defined. It is assumed, as in the mass law, that the structure has negligible stiffness and the stiffness matrix is expressed as follows:

$$\boldsymbol{K_l} = \begin{bmatrix} \sum k_{r_n} & -k_{r_1} & \cdots & -k_{r_n} \\ -k_{r_1} & k_{r_1} & \cdots & 0 \\ \vdots & \vdots & \ddots & \cdots \\ -k_{r_n} & 0 & 0 & k_{r_n} \end{bmatrix}, \tag{15}$$

where k_{r_n} is stiffness of n_{th} resonator. The mass and stiffness matrices are used to calculate displacement d at an arbitrary point [16] according to the equation:

$$d(\omega) = (\boldsymbol{K_l} - \omega^2 \boldsymbol{M_l}). \tag{16}$$

The effective mass of the plate-LRS system is calculated as follows [8]:

$$m_T = \frac{F}{\ddot{x}} = \frac{F}{(-\omega^2 x)}, \tag{17}$$

where F is the force and x is the displacement. In TL calculation the unit force represents acoustic wave impinging on the plate structure. The effective mass per area S can be calculated and then substituted into equation (13) as follows:

$$TL_{LRS} = 20 \log \left[\frac{\pi f \frac{m_T}{S}}{\rho_a c_a} \right]. \tag{18}$$

4. Results and discussion

In this section, the simulations results are presented and discussed. Tab. 1 presents mechanical properties of the thin plate structure considered in this study. Firstly the dependencies between frequency ratio, mass ratio and the stopband wideness are presented and then the relationship between dispersion curves and transmission loss are confronted. Frequency ratio is defined as ratio of resonance frequency of LRS to Bragg frequency given in equation (7). Mass ratio is the ratio of LRS mass to mass of plain plate.

Tab. 1. Parameters of thin aluminium plate considered in this study.

Quantity	Symbol	Unit	Value
Density	ρ	kg/m^3	2700
Thickness of plate	h	m	0.001
Young modulus of plate	E	GPa	69
Poisson ratio	ν	-	0.33
Length of unit cell	L	m	0.03

In the Fig. 4 and Fig. 5 the relations between stopband bandwidth and added LRS mass and frequency are presented. In the Fig. 4 it can be observed, that the bandwidth grows with increasing mass of the LRS. If the frequency of LRS is equal to ω_B, the stopband appears only below Bragg frequency. If the resonator frequency is lower than Bragg frequency, the stopband is narrower, but it appears above and below resonance frequency symmetrically. In the Fig. 6 one can observe, how the bandwidth of stopband change for different resonance frequencies of the LRS. The smaller the ratio between resonance and Bragg frequency is, the smaller the stopband is. The ratio between mass of added resonators and mass of the plate is equal to 0.3 – the ratio is chosen as an example. The main reason for using locally resonant metamaterials is their lightweight, therefore in later experimental validation of these simulations weight of the added structures won't be higher than half of the weight of the plate.

In the Fig. 6 and Fig. 7 the relation between transmission loss and dispersion curves is presented. In both cases the unit cell length was 0.03 m and the resonators were tuned to 400 Hz. As it can be seen in the Fig. 6 the TL for plate with LRS is 40 dB higher than for plain plate but around 450 Hz the antiresonance appears and lowers the TL by about 20 dB. In the region where the negative resonance appears, the second eigenvalue appears for several directions in the dispersion curve in the Fig. 7. It can be assumed that resonance of LRS is connected with lower boundary of stopband in dispersion chart and the upper boundary determines the appearance of antiresonance.

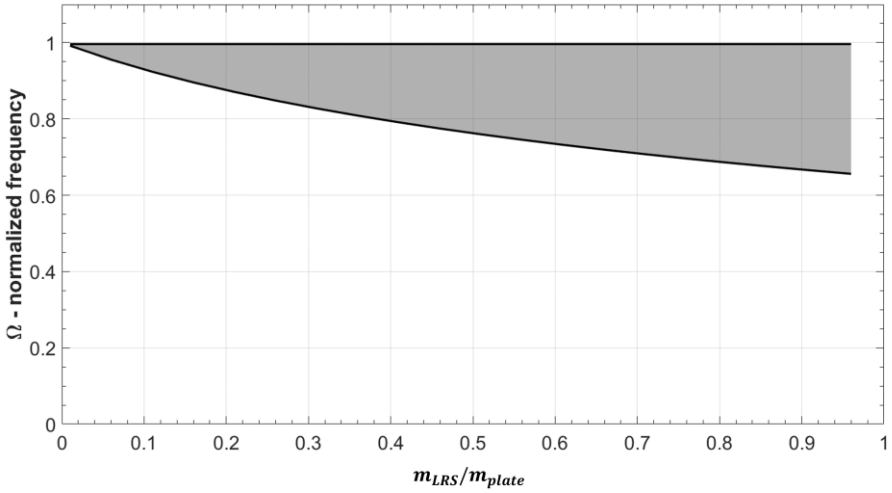

Fig. 4. Relation between mass ratio and stop band bandwidth for LRS tuned to $\omega_{LRS} = \omega_B$.

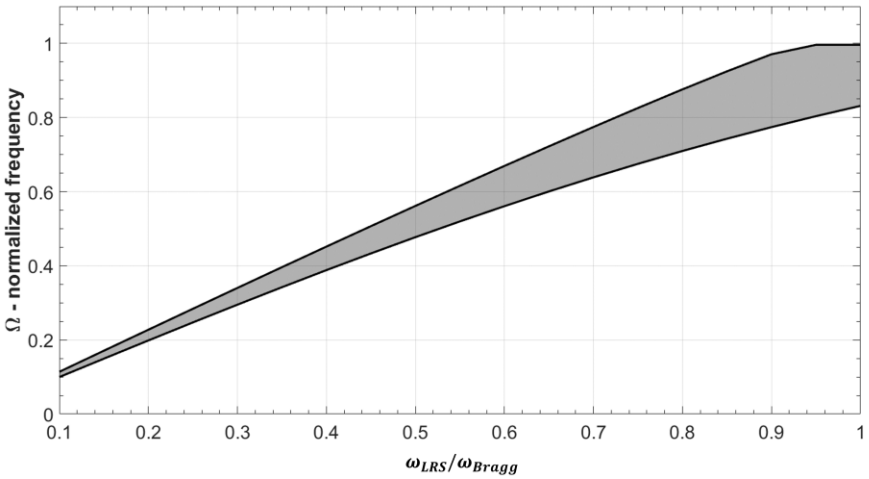

Fig. 5. Relation between frequency ratio and stop band bandwidth for LRS mass $m_{LRS} = 0.3m_{plate}$.

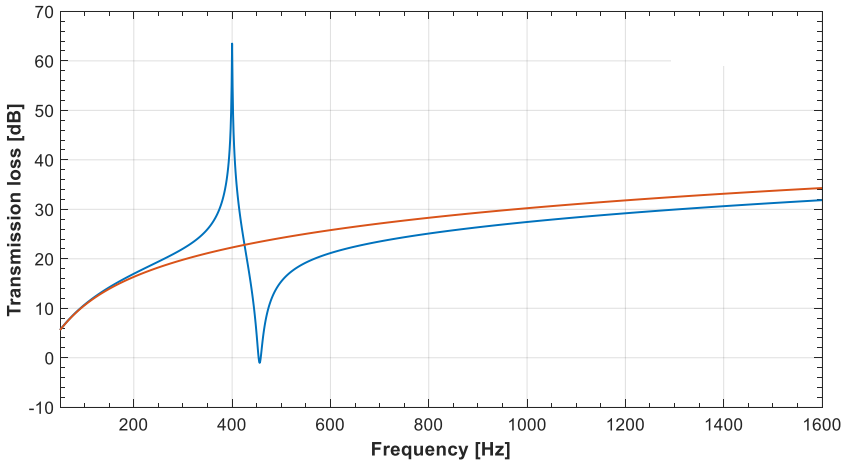

Fig. 6. Transmission loss for the plain plate structure (solid red line) and structure with added LRS (solid blue line).

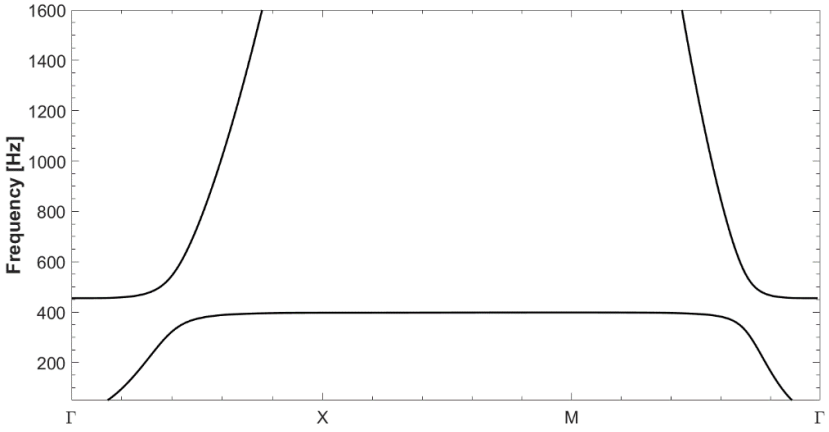

Fig. 7. Dispersion curves for unit cell $L = 0.03\ m$ and LRS tuned to 400 Hz.

5. Summary

This paper presents the potential of stop bands in suppressing wave propagation in certain frequency ranges determined by locally resonant structures. It is shown, that periodic addition of resonant mass-spring structure introduces the stop band effect in free wave propagation, which bandwidth is dependent from mass addition and ratio between Bragg and resonator frequency. The main limitation of periodic LRS is that stop band effect cannot be obtain above Bragg frequency, however with properly small length of unit cell Bragg frequency is high and for acoustic purposes, it does not create problems. The dispersion diagrams used for characterisation of flexural waves in the structure have impact on the sound transmission loss, when it comes to locally resonant structures. The local minimum and maximum in TL characteristics are directly connected with appearance of first and second eigenfrequency on the dispersion diagram.

In future work the acoustic measurement of sound transmission loss will be performed in order to validate the simulation results. The important site of future work would be realization of dispersion diagrams and TL simulations for 3D geometrical models.

References

1. Y. Tang, S. Ren, H. Meng, F. Xin, L. Huang, T. Chen, et al. Hybrid acoustic metamaterial as super absorber for broadband low-frequency sound. Sci. Rep., 7:43340, 2017.
2. S. Zuo, H. Huang, X. Wu, M. Zhang, T. Ni. Low-frequency band gap of locally resonant phononic crystals with a dual-base plate. J. Acoust. Soc. Am. ,143:1326–1332, 2018.
3. A. Hall, G. Dodd, E. Calius. Diffuse field measurements of Locally resonant partitions. Australian Acoustical Society Annual Conference (AAS2017), 1–10, 2017.
4. N. Jiménez, W. Huang, V. Romero-García, V. Pagneux, J.P. Groby. Ultra-thin metamaterial for perfect and quasi-omnidirectional sound absorption. Appl. Phys. Lett., 109:12902, 2016.
5. C.C. Claeys, K. Vergote, P. Sas, W. Desmet. On the potential of tuned resonators to obtain low-frequency vibrational stop bands in periodic panels. J. Sound Vib., 332(6):1418–1436, 2013.
6. L. Brillouin. Wave propagation in periodic structures: electric filters and crystal lattices. 1953.
7. F.A. Pires, L. Sangiuliano, H. Denayer, E. Deckers, C. Claeys, W. Desmet. Suppression of flow-induced noise and vibrations by locally resonant metamaterials. Aiaa Aviat. 2020 Forum, 1–10, 2020.
8. A.J. Hall, G. Dodd, E.P. Calius. Multiplying resonances for attenuation in mechanical metamaterials: Part 1 – Concepts, initial validation and single layer structures. Appl. Acoust., 170:107513, 2020. DOI: https://doi.org/10.1016/j.apacoust.2020.107513
9. C. Claeys, E. Deckers, B. Pluymers, W. Desmet. A lightweight vibro-acoustic metamaterial demonstrator: Numerical and experimental investigation. Mech. Syst. Signal Process., 70-71:853–880, 2016.
10. M. Zientek. Broadband vibration control through periodic arrays of locally resonant inclusions. PhD Thesis, Università degli Studi di Udine, 2018.

11. R. Szilard. Theories and applications of plate analysis: classical, numerical and engineering methods. Appl. Mech. Rev., 57(6):B32–B33, 2004.
12. G. De Abreu, J.F. Ribeiro, V. Steffen Jr. Finite element modeling of a plate with localized piezoelectric sensors and actuators. J. Brazilian Soc. Mech. Sci. Eng., 26(2):117–128, 2004.
13. M. Oudich, X. Zhou, M.B. Assouar. General analytical approach for sound transmission loss analysis through a thick metamaterial plate. Journal of Applied Physics, 116:193509, 2014.
14. L. Van Belle, W. Desmet. Damping in a locally resonant metamaterial using inverse and direct unit cell modelling. 11th International Congress on Engineered Materials Platforms for Novel Wave Phenomena – Metamaterials 2017, 364–366, 2017.
15. C. Valencia, J. Gomez, N. Guarín-Zapata. A general-purpose element-based approach to compute dispersion relations in periodic materials with existing finite element codes. J. Theor. Comput. Acoust. 28(3): 1950005, 2020.
16. A. Hall, E. Calius, G. Dodd, E. Wester, K. Chan. Development of locally resonant structures for sonic barriers. Build. Acoust., 21(3):199–220, 2014.

© 2021 by the Authors. Licensee Poznan University of Technology (Poznan, Poland). This article is an open access article distributed under the terms and conditions of the Creative Commons Attribution (CC BY) license (http://creativecommons.org/licenses/by/4.0/).